CHAPTER FOUR
LDV SCANNER CALIBRATION

ESDM ultimately determines velocity field direction using scan angles which define the laser beam direction at each registration and scan point. These angles depend upon computer-generated voltage signals that control scanner mirror deflection. Consequently, scanner calibration was necessary since it provided a mathematical expression describing this dependency. This chapter briefly describes the scanners installed in the particular LDV used to evaluate ESDM and the computer system which controls the scanners. The actual calibration procedure is discussed and the resulting expressions which define the scanner voltage signal/scan angle relationships for each scanner are presented.

Nomenclature

c	constant
E	voltage
h	distance from laser beam virtual origin to digitizer coordinate system origin
l	distance from laser beam virtual origin to point illuminated by laser beam
n	numer of DAC steps
s	distance from digitizer coordinate system origin to point illuminted by laser beam
SNR	signal-to-noise ratio
x_L, y_L, z_L	spatial LDV coordinate system Cartesian coordinates
θ	general scan angle
θ_H	horizontal scan angle
θ_V	vertical scan angle
$\hat{\theta}_H$	regressed horizontal scan angle
$\hat{\theta}_V$	regressed vertical scan angle
σ	scan angle residual variance
μ	scan angle residual mean
μ_h	uncertainty associated with h

μ_l uncertainty associated with l
μ_s uncertainty associated with s
μ_θ uncertainty associated with θ
ϕ angle between h and s

Scanner Description

The LDV, pictured in Fig. 5 and manufactured by Ometron[1], utilizes two orthogonally oriented General Scanning[2] model 325DT scanners which deflect the laser

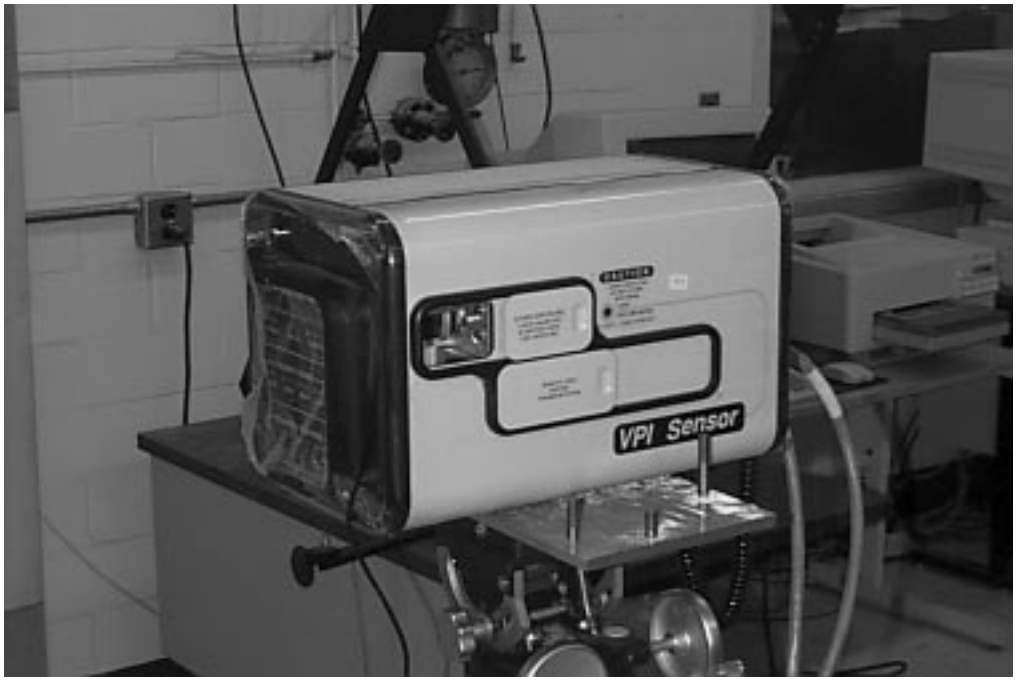

Figure 5. Ometron LDV

beam horizontally and vertically. Each scanner is composed of a mirror and a rotational galvanometer as depicted in Fig. 6. Considering Fig. 7, rotation of the bottom scanner mirror deflects the laser beam horizontally along the top mirror yielding horizontal movement of the laser beam and rotation of the top scanner mirror deflects the laser beam

[1] Ometron, Ltd., Kelvin House, Worsley Bridge Road, London SE26 5BX United Kingdom
[2] General Scanning, Inc., 500 Arsenal Street, Watertown, MA 02172

vertically. Henceforth, the bottom scanner is referred to as the horizontal scanner and the top scanner is referred to as the vertical scanner. The scanners are independently controlled by externally applied analog voltage signals which range ±5 V. The maximum

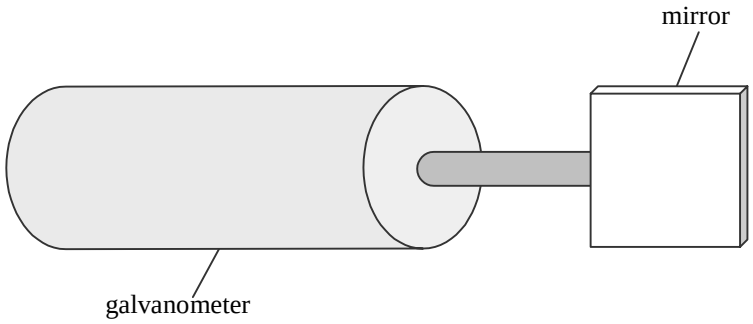

Figure 6. Scanner components

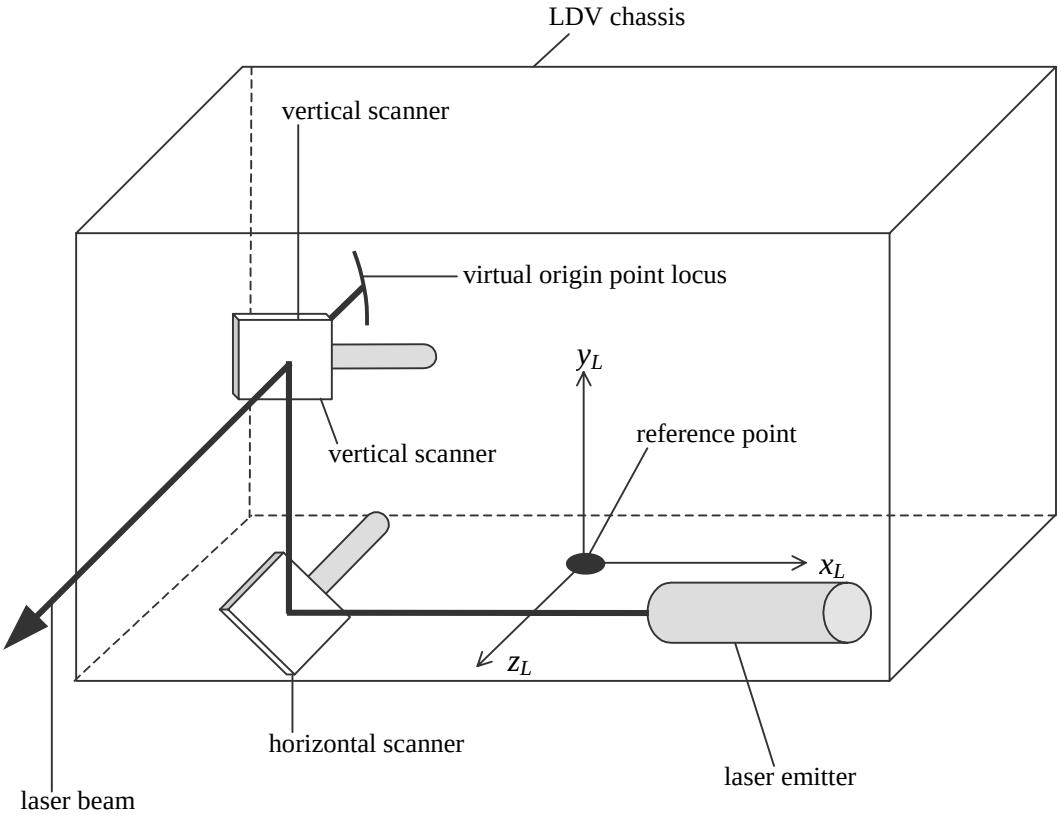

Figure 7. Scanner mounting configuration

rotation for either mirror is 25°; hence the horizontal and vertical scan angles range ±12.5°.

Figure 7 also shows the chassis location which serves as the fixed reference point for the LDV optics and the origin of the LDV coordinate system used by ESDM. The reference point coincides with the center of a threaded base insert which allows the LDV to be mounted on a standard tripod. The horizontal and vertical scanner mirror axes are referenced to this location. Therefore, the location of the laser beam virtual origin with respect to the reference point is known for any horizontal and vertical scanner mirror rotation. When both mirrors are rotated, the virtual laser origin traces an arc with a center at the vertical mirror center and a radius equal to the vertical separation distance between the two mirrors. As illustrated in Fig. 7 for arbitrary horizontal and vertical scanner mirror rotations, the laser beam virtual origin traces an arc in the y_L-z_L plane described by the following coordinates [36]:

$$\begin{Bmatrix} x_L \\ y_L \\ z_L \end{Bmatrix} = \begin{Bmatrix} -5.31 \\ 6.02 + 1.8\sin\theta_V \\ 2.6 - 1.8\cos\theta_V \end{Bmatrix} \text{ in } \left(\begin{Bmatrix} \text{-135} \\ 153 + 46\sin\theta_V \\ 67 - 46\cos\theta_V \end{Bmatrix} \text{ mm} \right) \tag{87}$$

where θ_V, in radians, is the resulting vertical scan angle corresponding to vertical mirror rotation. If only the bottom mirror is rotated, the laser beam virtual origin is located at a stationary point behind the vertical mirror centerline at a distance equal to the separation between the horizontal and vertical mirrors. For this case, the vertical scan angle is zero; hence the laser beam virtual origin is located at

$$\begin{Bmatrix} x_L \\ y_L \\ z_L \end{Bmatrix} = \begin{Bmatrix} -5.31 \\ 6.02 \\ 0.83 \end{Bmatrix} \text{ in } \left(\begin{Bmatrix} -135 \\ 153 \\ 21 \end{Bmatrix} \text{ mm } \right). \tag{88}$$

If only the vertical scanner mirror is rotated with the horizontal mirror maintained at zero, the laser beam virtual origin degenerates to the vertical mirror centerline [37]. For this case, the laser beam virtual origin is located at [38]

$$\begin{Bmatrix} x_L \\ y_L \\ z_L \end{Bmatrix} = \begin{Bmatrix} -5.31 \\ 6.02 \\ 2.6 \end{Bmatrix} \text{ in } \left(\begin{Bmatrix} -135 \\ 153 \\ 67 \end{Bmatrix} \text{ mm } \right). \tag{89}$$

Each of the three previous equations neglects the fact that the mirror reflective surface for each scanner does not coincide with the axis of rotation. Each mirror reflective surface is offset approximately 0.1 in. (3 mm) from the center of rotation to optimize the dynamic response of the scanner. However, Li [39] showed that this offset does not significantly affect the manner in which scan angles are determined. Thus, the offset was neglected.

Scanner Control System

The LDV scanner control system is schematically depicted in Fig. 8. Separate digital signals for each scanner are generated by software installed on a Silicon Graphics[3] Crimson® workstation. A certain number of integer digital-to-analog conversion (DAC) steps form each digital command. The digital commands are transformed into analog voltage signals by an IOtech[4] model DAC 488/4 digital-to-analog (D/A) converter. The LDV scanners accept analog voltages which range ±5 V. The digital voltage commands

[3] Silicon Graphics, Inc., 2011 North Shoreline Boulevard, Mountain View, CA 94043
[4] IOtech, Inc., 25971 Cannon Road, Cleveland, OH 44146

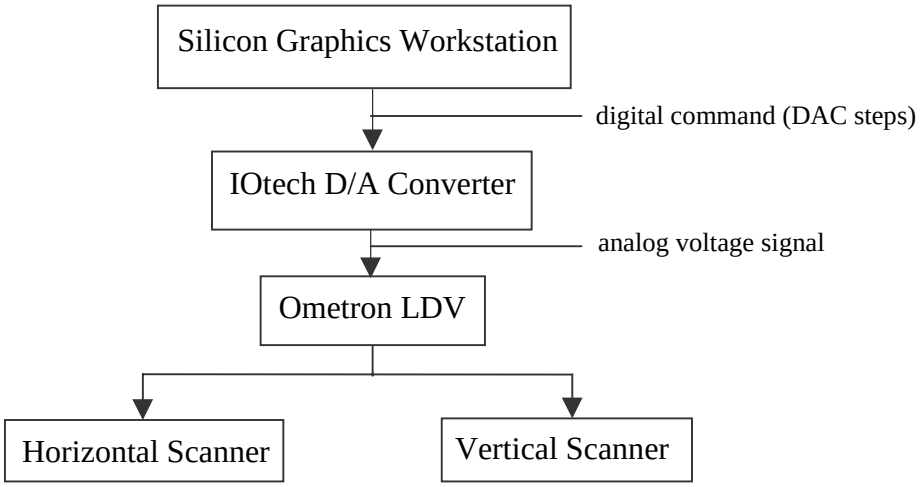

Figure 8. Scanner control system schematic

range ±4000 DAC steps. Therefore, the relationship between analog voltage and DAC steps is

$$E = \frac{10\ \text{V}}{8000} n = 1.25n\ \text{mV}, \tag{90}$$

where n is the number of DAC steps. The resulting analog voltage signals are sent to the LDV power supply which distributes each signal to the appropriate scanner.

Scanner Calibration Method: Analytical Approach

The scanners are ultimately controlled by externally applied, computer-generated digital commands. Consequently, the scan angles through which the laser beam is deflected are directly dependent upon these commands. Accurate velocity field reconstruction via ESDM requires precise knowledge of the scan angles since the direction cosines that define laser beam direction at each scan point are solely determined by the scan angles and the transformation matrix resulting from LDV registration. Moreover, the transformation matrix depends on the LDV coordinate system, which itself

is dependent upon the scan angles at each registration point. Therefore, accurate velocity field reconstruction requires extremely precise knowledge of the relationship between scanner voltage signals and resulting scan angles.

The relationship between scanner analog voltage signals and scan angles is nominally known. The nominal analog voltage range is 10 V corresponding to a ±5 V range and the maximum nominal scan angle deflection is 25°, or 436 mrad, horizontally and vertically. Therefore, the absolute linear relationship between either scan angle and corresponding scanner analog voltage signal is

$$\theta = \frac{436 \text{ mrad}}{10 \text{ V}} E = 43.6E \text{ mrad}, \tag{91}$$

where the scan angles are referenced to 0 V, implying the scanner voltage E varies ±5 V. Also, from Eqs. (90) and (91), the absolute linear relationship between either scan angle and corresponding DAC steps is

$$\theta = 55n \text{ μrad}. \tag{92}$$

However, these nominal expressions are not precise. The scanners exhibit maximum ±0.3% non-linear behavior within their range up to 50° [40]. Such non-linear behavior induces ESDM velocity field solution error. Thus, a more exact expression relating scanner voltage signals and resulting scan angles was necessary.

Zeng [41] formulated a LDV scanner calibration method based upon right-triangle relationships which can be used to obtain an expression relating scanner voltage signals and scan angles. The method first involves orienting the LDV such that the laser beam is perpendicular to a large, nominally flat surface at its home position. Again, the laser

beam home position is defined as the position at which the applied voltage to each scanner is zero; all scan angles are referenced to this home position. The distance from the laser virtual origin to the home position on the flat surface is recorded. Then, the laser beam is incrementally deflected through several horizontal or vertical scan angles depending on the scanner being calibrated. At each scan angle increment, the scanner digital commands and the analog voltage signals are recorded. Considering Fig. 9, each scan angle is calculated from the following general expression:

$$\theta = \tan^{-1}\left(\frac{s}{h}\right), \tag{93}$$

where θ is either a horizontal or vertical scan angle, s is the distance from the home position to the point on the flat surface illuminated by the laser beam at each scan angle increment and h is the distance from the LDV virtual origin to the home position. After voltage signals are recorded and Eq. (93) is evaluated at each scan angle increment, linear and quadratic regressions are performed yielding expressions which relate scanner digital

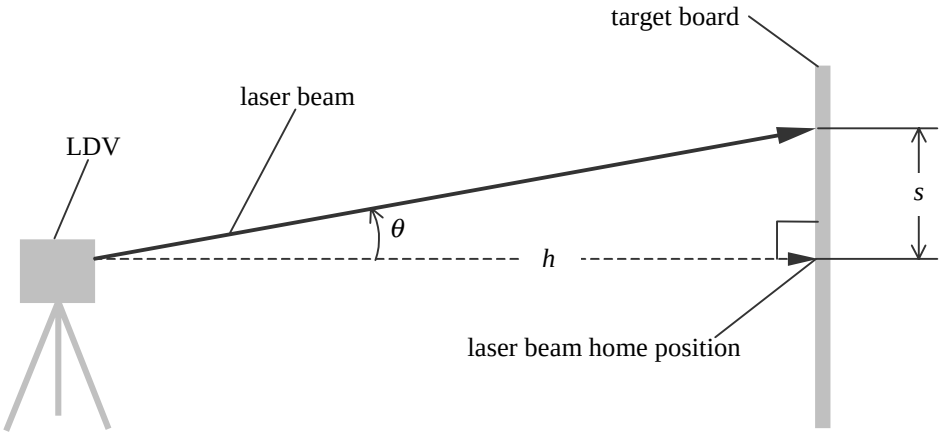

Figure 9. Scan angles calculated via right-triangle approach

voltage commands and analog voltage signals to the resulting scan angles.

Unfortunately, the scanner voltage signal/scan angle expressions obtained from this calibration method are subject to error. The primary error sources are associated with the use of right-triangle relationships to calculate scan angles. Achieving and maintaining perpendicularity between the laser beam at its home position and the flat surface is extremely difficult to achieve in practice. Hence, uncertainty is associated with any perpendicularity claim and error is introduced into all right-triangle relationships. Furthermore, the acquisition of a large flat surface is difficult. Thickness variations and bowing are present over any large surface area which introduce additional error into right-triangle relationships. Consequently, for this work, an improved calibration method was formulated which does not rely on right-triangle relationships.

Instead of using right-triangle relationships, the improved calibration method determines scan angles using cosine-law relationships. As before, the distance from the laser virtual origin to the home position is measured. Again, the laser beam is deflected through several horizontal or vertical scan angles depending on the scanner being calibrated. At each scan angle increment, scanner digital commands and analog voltage signals are recorded. Considering Fig. 10, scan angles are determined by the following general relationship based upon the cosine law:

$$\theta = \cos^{-1}\left(\frac{h^2 + l^2 - s^2}{2hl}\right), \tag{94}$$

where θ is either a horizontal or vertical scan angle, s is the distance from the home position to the point on the flat surface illuminated by the laser beam at each scan angle

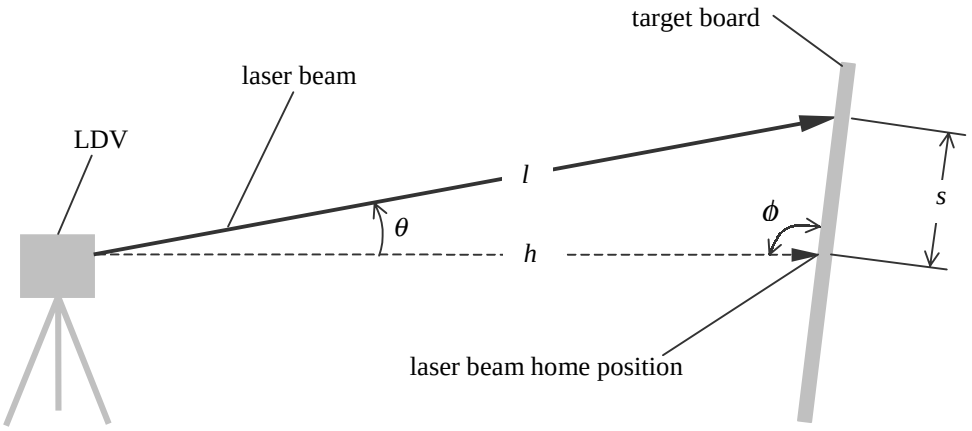

Figure 10. Scan angles calculated via cosine-law approach

increment, *h* is again the distance from the LDV virtual origin to the home position and *l* is the distance from the LDV virtual origin to the point illuminated by the laser beam. After voltage signals are recorded and Eq. (94) is evaluated at each scan angle increment, linear and quadratic regressions are performed yielding expressions which relate scanner digital commands and analog voltage signals to the resulting scan angles.

A cosine-law approach is desirable since it eliminates the need to establish perpendicularity between the flat surface and the laser beam at its home position. Moreover, a flat surface is not required if distances are measured with respect to a predefined three-dimensional coordinate system as opposed to direct measurements using, say, a tape measure or ruler. Thus, unlike the right-triangle approach, scan angle uncertainty associated with a perpendicularity claim is eliminated. Furthermore, scan angle uncertainty associated with a flat surface claim is eliminated if distances are measured indirectly with respect to a predefined coordinate system. Therefore, the

resulting scanner voltage signal/scan angle expressions are more precise and yield more accurate ESDM velocity field solutions.

Scanner Calibration Method: Experimental Procedure

The improved scanner calibration method was used to obtain scanner voltage signal/scan angle expressions for the horizontal and vertical scanners installed in the Ometron LDV. Figure 11 shows the experimental arrangement. An 8.0x5.0 ft (2.4x1.5 m) wood board with graph paper glued to one side was attached to a wall. A Modal Shop[5] model 5230XLD acoustic digitizer microphone array was placed near the board and the digitizer was calibrated. The digitizer was essential since it defined two three-dimensional Cartesian coordinate systems: one coordinate system for each of the horizontal and vertical scanner calibrations. In turn, these coordinate systems allowed indirect measurement of distance values in Eq. (94). Consequently, a flat surface was not required. Digitizer operation is described by its user manual [42]. The Ometron LDV was mounted on a tripod via the threaded-base insert and positioned approximately 11 ft (3.4 m) from the board. Again, the threaded-base insert served as the laser virtual origin reference point.

Initially, horizontal scanner voltage signal/horizontal scan angle expressions were obtained. First, the LDV and D/A converter were turned on at least three hours before the calibration procedure was initiated. This ensured that the LDV and D/A converter achieved steady-state thermal operating conditions. Second, the board was oriented such that its longest dimension was parallel to the floor. Third, the LDV was oriented by the

[5] The Modal Shop, Inc., 1776 Mentor Avenue, Suite 170, Cincinnati, OH 45212

tripod controls such that the laser home position was near the board center. Fourth, a coordinate system was defined by the digitizer.

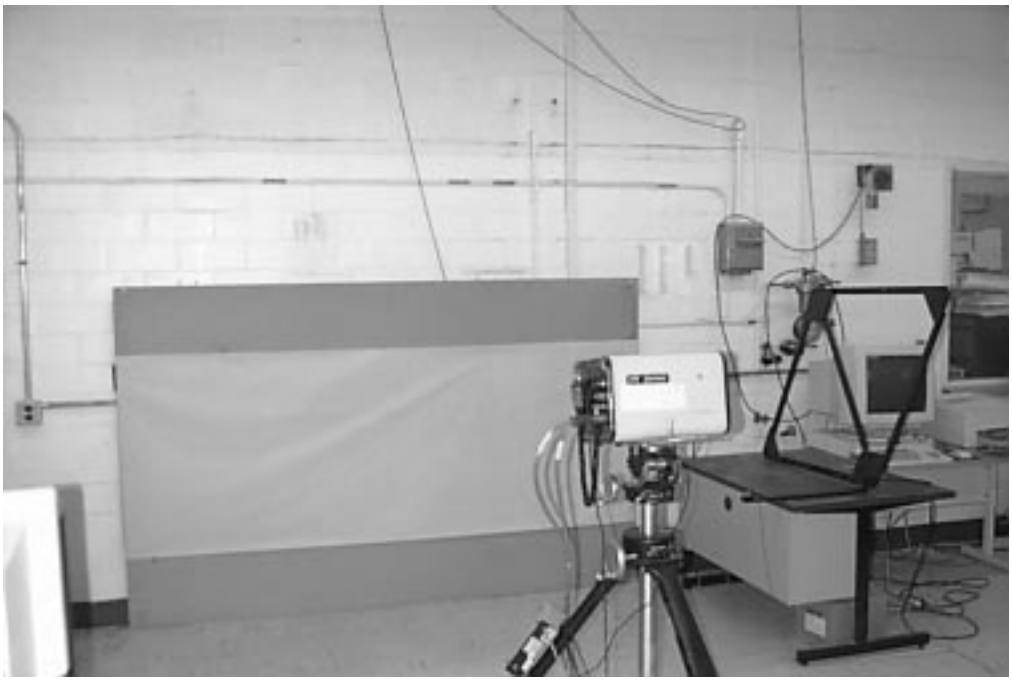

Figure 11. Experimental arrangement for improved LDV scanner calibration method

Fifth, the position coordinates of three steel pins secured to the aluminum plate inserted between the LDV and tripod mounting surface were recorded by the digitizer. Specifically, the position coordinates of the centers of the pin tips were recorded. The three pins and the aluminum plate attached to the LDV are pictured in Fig. 12. The pins were placed at fixed and known locations on the plate relative to the LDV coordinate origin; therefore, the position coordinates of the pin tips were also known in the LDV coordinate system. Consequently, the pin tips provided three non-collinear points which ultimately allowed the development of a transformation equation between LDV coordinates and the coordinate system defined by the digitizer. Subsequently, the

resulting transformation equation permitted the transformation of the laser virtual origin from LDV coordinates to the digitizer coordinate system. Mathematical development of the transformation equation is described in the Appendix.

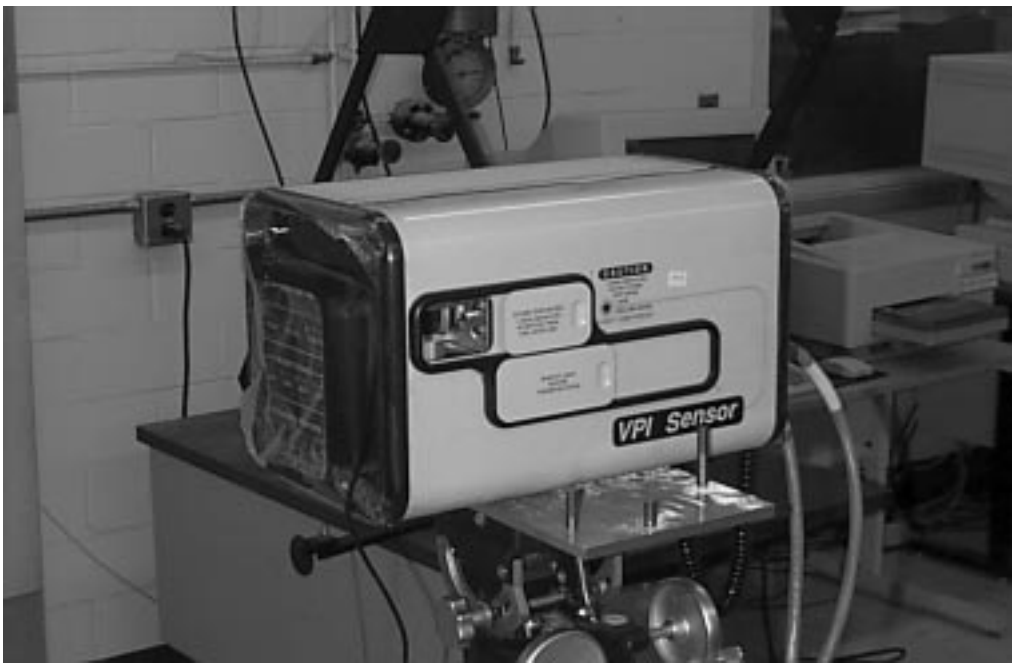

Figure 12. Aluminum plate with three pins

Sixth, the laser beam was sequentially deflected through twenty-one consecutive horizontal scan angles by progressing consecutively through DAC steps from –3500 to 3500 in 350 DAC step increments. At each DAC step increment, the corresponding analog voltage and position coordinates of the point on the board illuminated by the laser beam were recorded by the digitizer. The position on the board illuminated by the laser beam at 0 DAC step was the laser home position.

Seventh, a MATLAB®[6] program processed the coordinate information and calculated horizontal scan angles via Eq. (94). Eighth, the program performed linear and quadratic regressions between the horizontal scan angles and DAC steps and recorded analog voltage signals. These regressions yielded expressions which relate horizontal scanner digital commands and analog voltage signals to the resulting horizontal scan angles.

After calibration of the horizontal scanner was completed, calibration of the vertical scanner was performed. Essentially the same calibration procedure yielded expressions which relate vertical scanner digital voltage commands and analog voltage signals to the resulting vertical scan angles. The only difference between the two procedures is the board was rotated 90° from its position pictured in Fig. 11 such that its longest dimension was perpendicular to the floor. The same MATLAB® program processed coordinate information and calculated vertical scan angles via Eq. (94). Again, the program performed linear and quadratic regressions between the vertical scan angles and DAC steps and recorded analog voltage signals. These regressions yielded expressions which relate scanner digital commands and analog voltage signals to the resulting vertical scan angles.

Scanner Calibration Results

The horizontal scanner calibration procedure yielded the analog voltage data and horizontal scan angle values listed in Table A1 in the Appendix. Linear and quadratic regressions between DAC step increments and horizontal scan angle values yielded

[6] MATLAB®, The MathWorks, Inc., Cochituate Place, 24 Prime Park Way, Natick, MA 01760

$$\hat{\theta}_H = (-53.6n - 82.1)\ \mu\text{rad} \tag{95}$$

and

$$\hat{\theta}_H = (8.19\text{x}10^{-6} n^2 - 53.6n - 119)\ \mu\text{rad}, \tag{96}$$

respectively. From Eq. (92) after accounting for the correct sign, the nominal relationship between DAC steps and horizontal scan angles is

$$\theta_H = -55n\ \mu\text{rad}. \tag{97}$$

The linear term in Eqs. (95) and (96) compares favorably with Eq. (97). Figure 13 shows residuals between horizontal scan angle data and the regressed horizontal scan angle values at each DAC step increment. As previously cited, General Scanning specifies 0.3% non-linear behavior at 50°; this implies a maximum 2620 μrad scan angle residual. None of the residuals in Fig. 13 exceed this value; however, the horizontal scanner was only deflected about ±12°, not ±50°. Table 1 lists statistical properties associated with each residual set; the signal-to-noise ratio (SNR) is [43]

$$\text{SNR} = \frac{\max(\theta_H)}{\sigma}, \tag{98}$$

where max(θ_H) is the maximum calculated horizontal scan angle obtained from Eq. (94) and σ is the residual variance. The variance, standard deviation and SNR values listed in Table 1 quantitatively indicate that the quadratic regression yielded the slightly more accurate relationship between DAC steps and horizontal scan angle values.

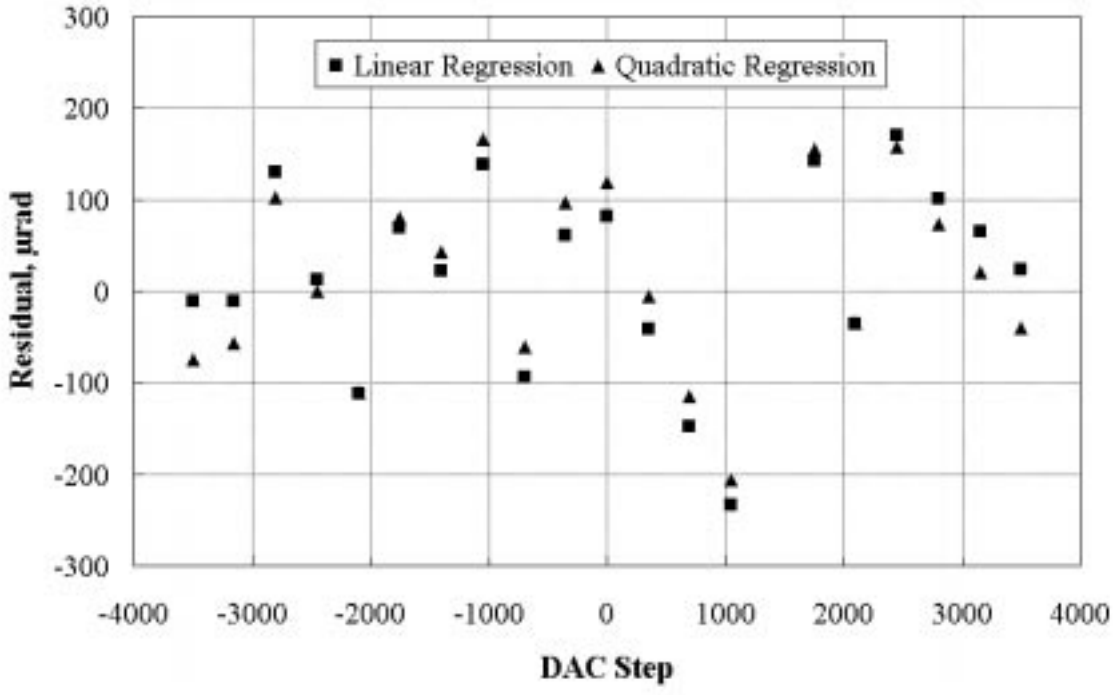

Figure 13. Horizontal scan angle residuals between horizontal scan angle data and regressed horizontal scan angle values at each DAC step increment

Table 1. Statistical properties associated with residuals between horizontal scan angle data and regressed horizontal scan angle values obtained from Eqs. (95) and (96) at each DAC step increment

Regression	Mean, μ μrad	Variance, σ^2 $(\mu\text{rad})^2$	Standard Deviation, σ μrad	SNR
Linear	$8.18\text{x}10^{-12}$	162	12.7	1474
Quadratic	$2.64\text{x}10^{-12}$	151	12.3	1528

Similarly, linear and quadratic regressions between analog voltage and horizontal scan angle data yielded

$$\hat{\theta}_H = \left(-42.9E - 8.27\text{x}10^{-2}\right) \text{ mrad} \tag{99}$$

and

$$\hat{\theta}_H = \left(5.09\text{x}10^{-4} E^2 - 42.9E - 0.118\right) \text{ mrad}, \tag{100}$$

respectively, where E is in units of volts. From Eq. (91) after accounting for the correct sign, the nominal relationship between analog voltage and horizontal scan angles is

$$\theta_H = -43.6E \text{ mrad}. \tag{101}$$

The linear term in Eqs. (99) and (100) compares favorably with Eq. (101). Figure 14 shows horizontal scan angle residuals evaluated at each analog voltage value. As expected, none of the residuals in Fig. 14 exceed the 2620 μrad maximum residual value. Table 2 lists statistical properties associated with each residual set. The variance, standard deviation and SNR values listed in Table 2 closely approximate the corresponding values listed in Table 1. Again, the quadratic regression yielded the slightly more accurate relationship between analog voltage and horizontal scan angle data.

Table 2. Statistical properties associated with residuals between horizontal scan angle data and regressed horizontal scan angles obtained from Eqs. (99) and (100) at each recorded analog voltage

Regression	**Mean, μ mrad**	**Variance, σ^2 (μrad)^2**	**Standard Deviation, σ μrad**	**SNR**
Linear	$6.80\text{x}10^{-15}$	183	13.5	1389
Quadratic	$-1.92\text{x}10^{-13}$	172	13.1	1431

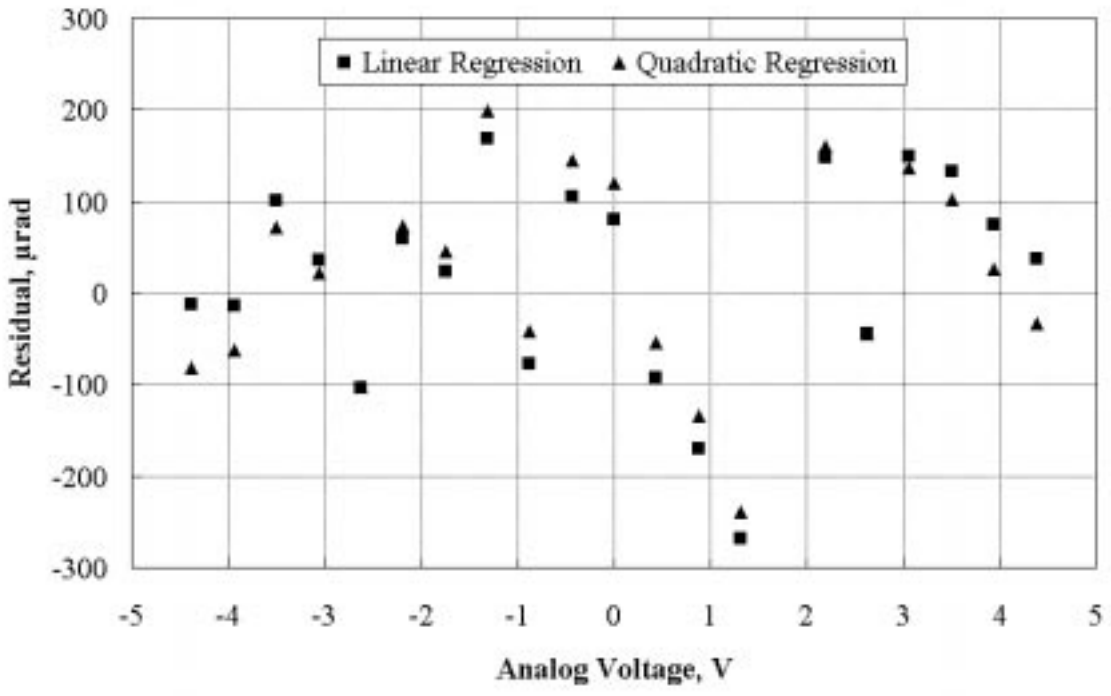

Figure 14. Horizontal scan angle residuals between horizontal scan angle data and regressed horizontal scan angle values at each recorded analog voltage

The vertical scanner calibration procedure yielded the analog voltage and scan angle data listed in Table A1 in the Appendix. Linear and quadratic regressions between DAC steps and vertical scan angle data yielded

$$\hat{\theta}_V = (55.8n - 165)\ \mu\text{rad} \tag{102}$$

and

$$\hat{\theta}_V = \left(-4.49\text{x}10^{-5} n^2 + 55.8n + 36.4\right)\ \mu\text{rad}, \tag{103}$$

respectively. The nominal relationship between DAC steps and vertical scan angles is

$$\theta_V = 55n\ \mu\text{rad}. \tag{104}$$

The linear term in Eqs. (102) and (103) agrees with Eq. (104). Figure 15 shows residuals between vertical scan angle data and the regressed vertical scan angles at each DAC step increment. None of the residuals in Fig. 15 exceed the 2620 μrad maximum residual value. However, these residuals are slightly higher than the horizontal scan angle residuals shown in Fig. 13, indicating that the vertical scanner exhibits slightly more non-linear behavior than the horizontal scanner. Also, the residuals resulting from the linear regression exhibit a slight deterministic relationship in the form of an inverted parabola. This phenomena was observed before by Li [44] for a different model scanner from General Scanning and is attributable to errors associated with mounting of the galvanometer rotary position transducer within the vertical scanner [45]. Table 3 lists statistical properties associated with each residual set; the SNR now is

$$\text{SNR} = \frac{\max(\theta_V)}{\sigma}, \tag{105}$$

where $\max(\theta_V)$ is the maximum calculated vertical scan angle. The variance, standard deviation and SNR values listed in Table 3 clearly demonstrate that the quadratic regression yielded the more accurate relationship between DAC steps and vertical scan angle data.

Table 3. Statistical properties associated with residuals between vertical scan angle data and regressed vertical scan angle values obtained from Eqs. (102) and (103) at each DAC step increment

Regression	**Mean, μ μrad**	**Variance, σ^2 $(\text{mrad})^2$**	**Standard Deviation, σ (μrad)**	**SNR**
Linear	$-1.17\text{x}10^{-11}$	$45.8\text{x}10^{-2}$	214	915
Quadratic	$5.25\text{x}10^{-12}$	$11.9\text{xj}10^{-2}$	109	1795

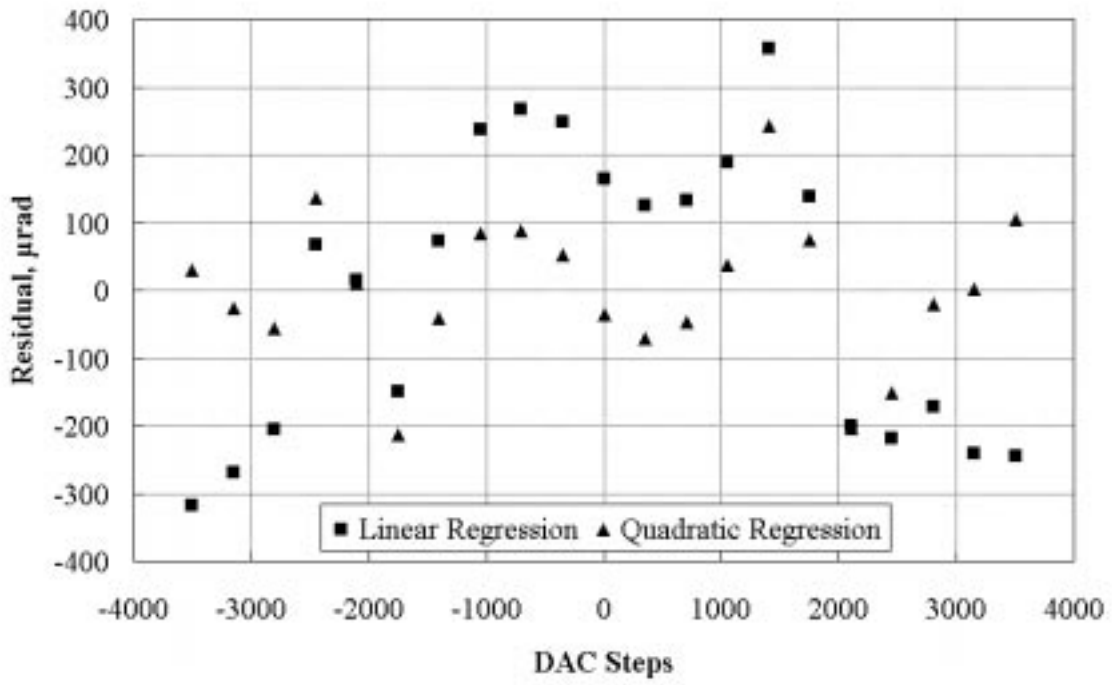

Figure 15. Vertical scan angle residuals between horizontal scan angle data and regressed horizontal scan angle values at each DAC step increment

Similarly, linear and quadratic regressions between recorded analog voltage and vertical scan angle data yielded

$$\hat{\theta}_V = \left(44.6E - 0.178\right) \text{ mrad} \tag{106}$$

and

$$\hat{\theta}_V = \left(-2.87\text{x}10^{-2} E^2 + 44.6E + 2.42\text{x}10^{-2}\right) \text{ mrad}, \tag{107}$$

respectively, where E is in units of volts. Again, the nominal relationship between analog voltage signals and horizontal scan angles is

$$\theta_V = 43.6E \text{ mrad}. \tag{108}$$

Considering the linear term in Eqs. (99) and (100) for the horizontal scan angles, the linear term in Eqs. (106) and (107) compares extremely well with Eq. (108). Figure 16 shows residuals between vertical scan angle data and the regressed vertical scan angle values. As expected, none of the residuals in Fig. 16 exceed the 2620 μrad maximum residual value, although these residuals are again higher than the horizontal scan angle residuals shown in Fig. 13. Table 4 lists statistical properties associated with each residual set. The variance, standard deviation and SNR values listed in Table 4 closely approximate the corresponding values listed in Table 3. Again, the quadratic regression clearly yielded the more accurate relationship between analog voltage and vertical scan angle data.

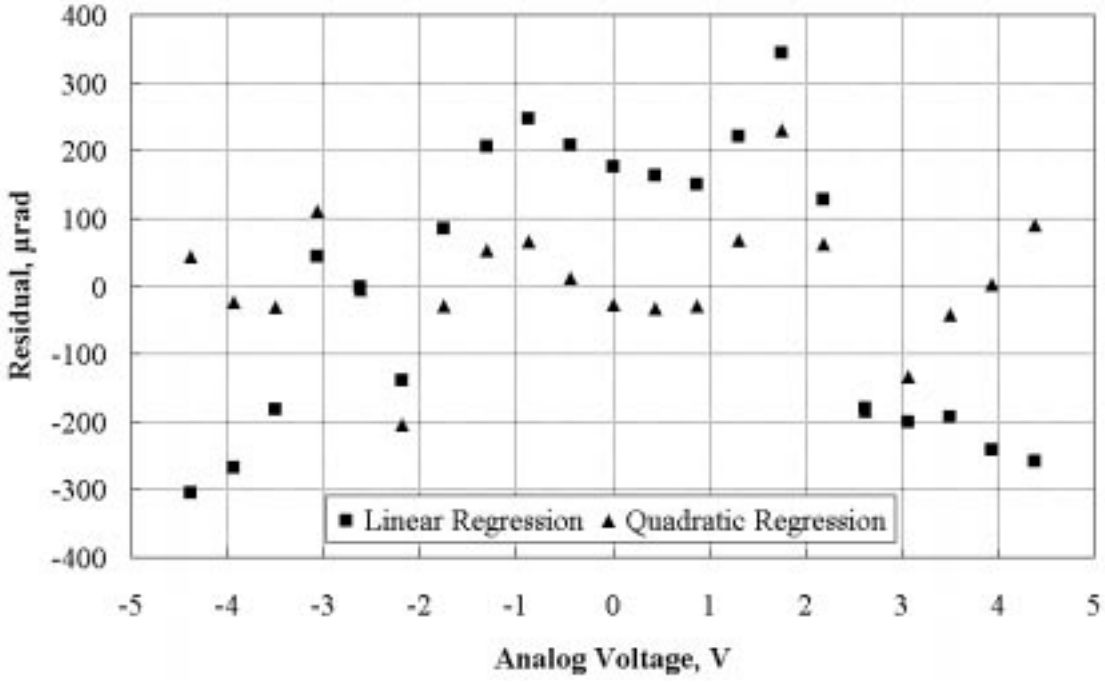

Figure 16. Vertical scan angle residuals between horizontal scan angle data and regressed horizontal scan angle values at each recorded analog voltage value

Table 4. Statistical properties associated with residuals between vertical scan angle data and regressed vertical scan angles obtained from Eqs. (106) and (107) at each recorded analog voltage

Regression	Mean, μ μrad	Variance, σ^2 $(\text{mrad})^2$	Standard Deviation, σ (μrad)	SNR
Linear	$-6.77\text{x}10^{-12}$	$43.5\text{x}10^{-2}$	209	939
Quadratic	$6.21\text{x}10^{-12}$	$9.56\text{x}10^{-2}$	97.8	2004

The scan angles calculated via Eq. (94) possess uncertainty which is present in the expressions obtained from the linear and quadratic regressions between scan angle and scanner voltage data. Such uncertainty emanates from the distance values in Eq. (94) which possess uncertainty associated with the digitizer. Based upon a first-order Taylor series expansion of Eq. (94), the scan angle uncertainty is [46]

$$\mu_\theta = \sqrt{\left(\frac{\partial\theta}{\partial h}\mu_h\right)^2 + \left(\frac{\partial\theta}{\partial l}\mu_l\right)^2 + \left(\frac{\partial\theta}{\partial s}\mu_s\right)^2}\,, \tag{109}$$

where μ_h, μ_l and μ_s are distance uncertainties associated with the distances h, l and s respectively. The partial derivatives in Eq. (109) are

$$\frac{\partial\theta}{\partial h} = \frac{l^2 + s^2 - h^2}{2hl^2\sqrt{1-c^2}}\,, \tag{110}$$

$$\frac{\partial\theta}{\partial l} = \frac{h^2 + s^2 - l^2}{2h^2 l\sqrt{1-c^2}} \tag{111}$$

and

$$\frac{\partial\theta}{\partial s} = \frac{s}{hl\sqrt{1-c^2}}\,, \tag{112}$$

where

$$c = \frac{h^2 + l^2 - s^2}{2hl}. \tag{113}$$

When the coordinates of the same point were repeatedly obtained by the digitizer, the average distance uncertainty observed was approximately 0.03 in. (1 mm). Therefore, the distances *h*, *l* and *s* in Eq. (94) had an average uncertainty of about 0.03 in. (1 mm); that is, for average uncertainty

$$\mu_h = \mu_l = \mu_s = 0.03 \text{ in } (1 \text{ mm}). \tag{114}$$

Another MATLAB® program was written which evaluated Eq. (109) using Eq. (114) for various *s* values with

$$h = 11 \text{ ft } (3.4 \text{ m}), \tag{115}$$

$$l = \sqrt{h^2 + s^2 - 2hs\cos\phi} \tag{116}$$

and assuming

$$\phi = 100°, \tag{117}$$

where ϕ is the angle between distances *h* and *s*.

Average scan angle uncertainty results are shown in Fig. 17. The results range between ±238 μrad and ±243 μrad and closely match the observed random variation, approximately ±250 μrad, exhibited by the scan angle residuals in Figs. 13-16. Therefore, the random variation of the scan angle residuals in Figs. 13-16 is most likely attributable to digitizer uncertainty.

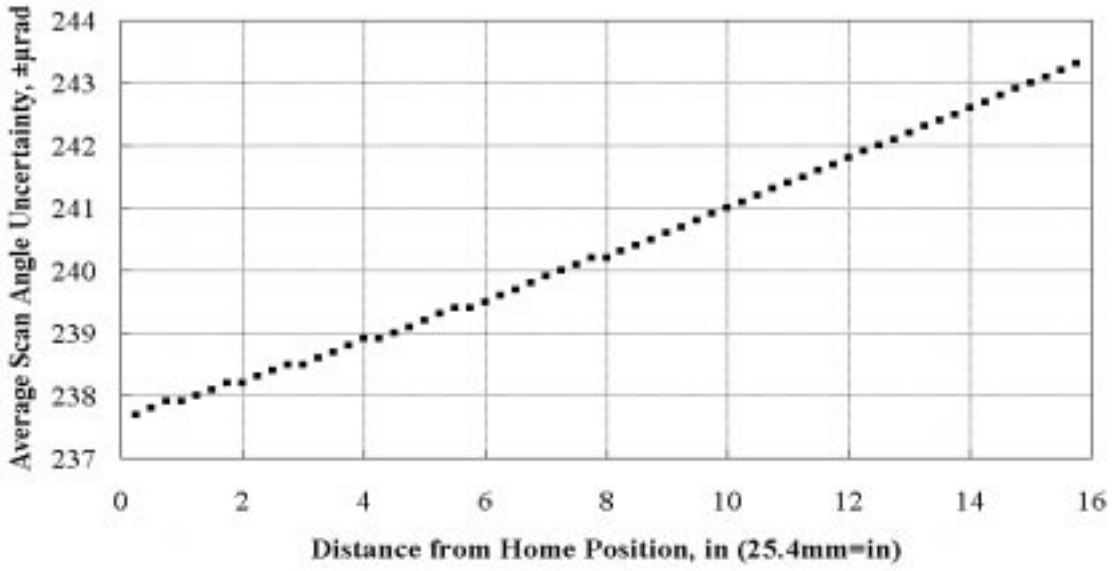

Figure 17. Estimated average horizontal and vertical scan angle uncertainty associated with LDV scanner calibration procedure based upon cosine-law approach at various distances from laser beam home position

Earlier ESDM software versions calculated scan angles using linear analog voltage scan angle expressions such as Eqs. (99) and (106). However, later versions calculate scan angles using more accurate quadratic scanner DAC step/scan angle expressions such as Eqs. (96) and (103). For this work, ESDM software calculated horizontal and vertical scan angles using Eqs. (96) and (103), respectively.